

Accelerometry-based classification of circulatory states during out-of-hospital cardiac arrest

Wolfgang J. Kern^{1,2}, Simon Orlob^{2,3,4}, Andreas Bohn^{5,6}, Wolfgang Toller³, Jan Wnent^{4,7,8}, Jan-Thorsten Gräsner^{4,7}, and Martin Holler^{1,2}

¹*Institute of Mathematics and Scientific Computing, University of Graz, Heinrichstraße 36, 8010 Graz, Austria*

²*BioTechMed-Graz, Graz, Austria*

³*Medical University of Graz, Department of Anesthesiology and Intensive Care Medicine, Division of Anesthesiology for Cardiovascular and Thoracic Surgery and Intensive Care Medicine, Graz, Austria*

⁴*University Hospital Schleswig-Holstein, Institute for Emergency Medicine, Kiel, Germany*

⁵*City of Münster Fire Department, Münster, Germany*

⁶*University Hospital Münster, Department of Anesthesiology, Intensive Care and Pain Medicine, Münster, Germany*

⁷*University Hospital Schleswig-Holstein, Department of Anaesthesiology and Intensive Care Medicine, Kiel, Germany*

⁸*University of Namibia, School of Medicine, Windhoek, Namibia*

May 16, 2022

Abstract

Objective: During cardiac arrest treatment, a reliable detection of spontaneous circulation, usually performed by manual pulse checks, is both vital for patient survival and practically challenging. Methods: We developed a machine learning algorithm to automatically predict the circulatory state during cardiac arrest treatment from 4-second-long snippets of accelerometry and electrocardiogram data from real-world defibrillator records. The algorithm was trained based on 917 cases from the German Resuscitation Registry, for which ground truth labels were created by a manual annotation of physicians. It uses a kernelized Support Vector Machine classifier based on 14 features, which partially reflect the correlation between accelerometry and electrocardiogram data. Results: On a test data set, the proposed algorithm exhibits an accuracy of 94.4 (93.6, 95.2)%, a sensitivity of 95.0 (93.9, 96.1)%, and a specificity of 93.9 (92.7, 95.1)%. Conclusion and significance: In application, the algorithm may be used to simplify retrospective annotation for quality management and, moreover, to support clinicians to assess circulatory state during cardiac arrest treatment.

1 Introduction

Cardiac arrest is one of the leading causes of death in the western world [1] with more than 400 000 resuscitation attempts by emergency medical services (EMS) per year in Europe alone [1]. High-quality cardiopulmonary resuscitation (CPR) - ensuring minimal circulation - along with defibrillation is the basic treatment EMS provide for patients with cardiac arrest. The objective of the treatment is a restoration of spontaneous circulation. However, recognizing a return of spontaneous circulation (ROSC) during brief rhythm checks is still a demanding task. Currently,

health-care providers check for mechanical activity of the heart by manual palpation of central pulses when the electrocardiogram (ECG) shows a potential perfusing rhythm. Manual pulse palpation has two big disadvantages: It often leads to long interruptions of CPR [2] and is highly error-prone [3]. Erroneous identification of spontaneous circulation leads to inadequate treatment by delaying chest compression and, consequently, decreases the patient’s survival probability [4] due to prolonged no-flow time. Physicians additionally employ endtidal CO₂-concentration levels and their trend as further information to augment the assessment of the circulatory state [5].

In the last two decades, various algorithms were proposed to classify the circulatory state during CPR. These algorithms employ ECG [6, 7], thoracic impedance [8, 9], combinations of those [10, 11, 12] and additionally capnography [13] or photoplethysmography [14] for classification, or are based on Doppler ultrasound [15]. These works focus mostly on the differentiation between pulse generating perfusing rhythms (PR) and pulseless electric activity (PEA), and some are subclassifying the latter into pseudo-PEA, and true-PEA. All these classes exhibit organized-looking ECG rhythms with the potential to generate a cardiac contraction, but differ in terms of cardiac output which is sufficient for PR, insufficient for pseudo-PEA and lacking for true-PEA, respectively. Thus, electro-mechanical coupling is present for PR and absent for PEA. For other ECG rhythms, the cardiac arrest is reliably diagnosable from ECG signal only.

During CPR, accelerometers are placed on the patient’s chest as feedback devices for the EMS delivering chest compressions. Inspired by the long-known technique of palpating the apex beat on the chest wall, these accelerometers were recently investigated on their capability to detect motions of the heart propagated to the chest wall to provide complimentary information about the mechanical activity of the heart. A proof of concept of this idea was provided in porcine models [16] and with smartphone-seismocardiography in humans [17], where the latter one focused only on the discrimination of the signals by blinded observers, while [16] proposed classifiers only on a single feature. However, a machine-learning-based automatic solution for determining the circulatory state of the heart from accelerometer data does not exist so far. To the best of our knowledge, this is the first work to address this problem by developing a machine-learning algorithm on real-world accelerometry (ACC) and ECG data of cardiac arrest.

2 Methods

2.1 Data collection and labeling

This study was approved by the ethics committee of the University of Kiel (Ref. no.: D 421/21) and the scientific advisory board of the German Resuscitation Registry (Ref. no.: AZ 2021-03). A sample of 917 cases with defibrillator records, all ZOLL X-Series (ZOLL Medical Corporation, Chelmsford, Massachusetts, United States), from the years 2013 to 2021 was obtained from the German Resuscitation Registry. All recordings were annotated retrospectively by an experienced physician (SO), utilizing an interactive, web-based plotting tool that we developed for this study using jupyter notebooks [18]. Cases recorded in the year 2020 were annotated independently by two experienced physicians, and dissenting annotations were resolved in consensus. The annotation consists of the determination of the start and the end of the resuscitation episode, including all ROSCs and rearrests which occur in this interval [19]. The physicians used ECG, ACC and, if available, capnography and non-invasive blood pressure for the labeling. Ambiguous situations were annotated assuming the treating physician followed the guidelines faultlessly. Nevertheless, obtuse intervals could be excluded from the subsequent analysis by a respective label from the annotators. These annotations form the ground truth in our data set.

After resampling ECG and ACC to $f_s = 250$ Hz for all cases, only the parts of the recordings with simultaneously given ACC, ECG, and capnography signals were used further. We require

the presence of capnography data since these provide at least some hemodynamic information for the retrospective annotation process. Furthermore, the signal after the last recorded period of chest compressions was excluded since it contains either mainly the patient’s transport to the hospital with potentially large artifacts or a low amplitude signal in ECG and ACC after death pronouncement, where circulation classification is clinically irrelevant. For the remaining signal parts, the algorithm described in [20, 21] was used to determine the periods where no chest compressions are present. From these periods, we extracted snippets with a length of 4 seconds, each one containing the ACC, ECG, and capnography signals and a label (‘Cardiac Arrest’ (AR) or ‘Spontaneous Circulation’ (SC)). The snippets are extracted in an overlapping way, cutting a 4-s-snippet every 2 seconds. These snippets form the database of our algorithm.

2.2 Preprocessing

We denote the ACC, ECG, and capnography signals of a snippet with N sample points as $a = (a_n)_n$, $e = (e_n)_n$ and $c = (c_n)_n$, where the indices n are such that $-N/2 \leq n < N/2$ respectively. We use \bar{d} to denote the mean $\bar{d} = (1/N) \sum_{n=-N/2}^{N/2-1} d_n$ of some signal d .

For all snippets we shift a and e so that they exhibit $\bar{a} = \bar{e} = 0$. To improve data quality of our snippets we impose the following constraints via a prefiltering step, which we refer to as *general prefiltering*: Constraining $\max |a_n| < 20$, $\max |e_n| < 2.5$ mV removes data with large artifacts and high amplitude noise, whereas $\max(|a_n|)/|\bar{a}| < 25$ and $\max(|e_n|)/|\bar{e}| < 35$ allow to identify and omit snippets with a sharply peaked artifact and thus corrupted signal like peaks from defibrillations in ECG or a sudden movement of the patient in ACC.

To further improve data quality, we optionally applied additional *capnography prefiltering* in our analysis to address one key limitation of the retrospective annotation process: The annotators employ only limited data as described in 2.1 to make their decision. Thus, an ultimate determination of the physiological state as ground truth remains impossible in some cases. Moreover, performing annotations with dichotomous labels to classify the circulatory state during cardiac arrest treatment is inevitably insufficient since cardiac output can vary continuously over time, and the data given are insufficient to differentiate between PR, pseudo-PEA, true-PEA reliably. In particular, the determination of the exact point in time of a (re-)arrest is challenging since this circulatory state transition from PR over pseudo-PEA to true-PEA sometimes takes place slowly, and determining an exact transition point unavoidable causes partially false labels in our ground truth. Thus, we employ capnography as hemodynamic information to include only unambiguous snippets by requiring $\max(c_n) < 20$ mmHg for snippets with label AR and $\max(c_n) > 30$ mmHg for SC-snippets. These thresholds were chosen as minimal constraints the respective circulatory states need to fulfill. Snippets not fulfilling these constraints might be falsely classified or are in a transition phase and are excluded.

2.3 Feature extraction

We extract several features from the ECG-signal e and acceleration signal a to use them as an input for the machine learning classifier. We use the mean absolutes $v_1 = \overline{|a_n|}$ and $v_2 = \overline{|e_n|}$ as features. To characterize the rhythmicity we employ the autocorrelation z_d of a real-valued signal d

$$z_d(k) = \frac{\sum_{n=-N/2}^{N/2-1} d_n d_{n+k}}{\sum_{n=-N/2}^{N/2-1} d_n^2}, \quad -N/2 \leq k < N/2, \quad (1)$$

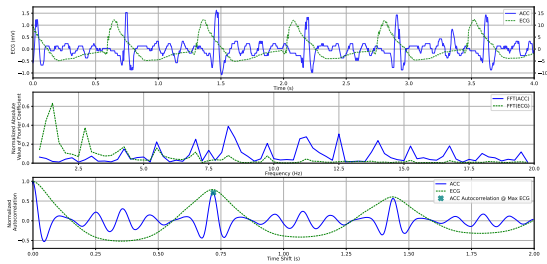


Figure 1: Exemplary Snippet. ACC and ECG signals are shown in the first subplot, their spectra in the second subplot. The autocorrelation is shown in the lowermost subplot. Even though one can see apparent acceleration excitation at the time of the QRS-complexes in ECG, the spectra exhibit different harmonics, leading to a small $v_5 = -0.037$. In contrast, the features based on the autocorrelation yield $v_6 = 0.712$ and $v_7 = -3040$ at the pronounced maximum at 0.7 s time shift.

where we zero-pad $(d_n)_n$ outside the defined range $-N/2 \leq n < N/2$. As usual $z_d(0) = 1$ holds, which we call the trivial maximum. We search for the largest nontrivial local maximum $z_d(\tilde{n}_d)$, $\tilde{n}_d \neq 0$. Its value $z_d(\tilde{n}_d)$ describes the rhythmicity of the signal, whereas \tilde{n}_d/f_s gives the time shift inducing highest self-similarity. We use the $v_3 = z_a(\tilde{n}_a)$ and $v_4 = z_e(\tilde{n}_e)$ as further input features. In order to describe the interdependence of a and e we use three different approaches:

- We compute the Fourier Transform of a and e and take the absolute values of the coefficients in the frequency band between 1 Hz and 20 Hz: $(s_a)_{i=1}^m$ and $(s_e)_{i=1}^m$. Then we take the correlation of these two vectors as a feature

$$v_5 = \frac{\sum_{i=1}^m s_{a_i} s_{e_i}}{\sqrt{\sum_{i=1}^m s_{a_i}^2 \sum_{i=1}^m s_{e_i}^2}}. \quad (2)$$

With this feature we aim to identify similar frequencies in both signals. However, as can be seen in Fig. 1, there are situations where different harmonics contribute to ECG and ACC spectra, leading to small values of v_5 even in case of clearly visible acceleration excitations following the QRS-complexes. Thus, this feature is insufficient to describe the interdependence.

- We employ the autocorrelation of the two signals (as shown in Fig. 1) to characterize the dependency of both signals further. We determine the shift \tilde{n}_e at which the nontrivial maximum of the ECG autocorrelation occurs and evaluate $v_6 := z_a(\tilde{n}_e)$. If the acceleration signal is influenced by the apex beat against the chest wall, we will observe simultaneous, rhythmic responses of the acceleration signal to this excitation represented by the QRS-complexes which correspond the electrical depolarization of the ventricles, ideally leading to a mechanical contraction with ejection of blood formatting a pulse wave. Thus z_a should exhibit a maximum at this shift if mechanical coupling is present, whereas we assume uncorrelated signals and therefore vanishing autocorrelation else.

Furthermore, we also use the second derivative $z_a''(n)$, approximated with finite stepsize $1/f_s$, to check the curvature of z_a at \tilde{n}_e . In case of mechanical coupling the curvature of z_a at the expected maximum \tilde{n}_e the should be negative. We use $v_7 = \overline{z_a''} := \frac{1}{5} \sum_{i=-2}^2 z_a''(n)|_{n=\tilde{n}_e+i}$ to include also neighboring curvature values. The highly generic properties of these features and their independence from any hyperparameters makes them very stable in application.

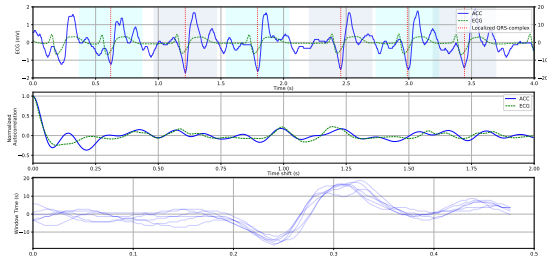


Figure 2: Exemplary Snippet. ACC and ECG signals are shown in the first subplot, their autocorrelation in the second subplot. Even though one can see clear ACC excitations at the time of the QRS-complexes in ECG, the autocorrelation maxima remain small due to arrhythmia: $v_6 = 0.089$ and $v_7 = 8.49$. Windows of fixed size localized around QRS-complexes are shown alternatingly in different pale shades of blue. The accelerometer signals during these windows are superimposed in the lowermost subplot, which reveals the high similarity. The feature based on the correlation of the windowed acceleration signals yields $v_8 = 0.898$.

- In case of arrhythmic ECG rhythms (e.g. atrial fibrillation, ventricular extrasystole), the methods relying on the autocorrelation fail, since there is no unique shift, for which the whole snippet is highly self-similar, even though characteristic acceleration patterns can still be associated to QRS-complexes (see Fig 2). To address this problem, we localize the QRS complexes similarly to the calculation of n_P as described in [22] by detecting their steep slopes: After applying a broad 5-th order Butterworth bandpass filter with limiting frequencies 0.5 and 30 Hz to e_n , we take the a 0.1-second-rolling-mean of the square of first difference

$$\overline{(e_{n+1}^{(filt)} - e_n^{(filt)})^2}_{0.1}, \quad (3)$$

normalize it by dividing it through its maximum and find the local maxima which exceed 0.33. The resulting candidates are further filtered by requiring different QRS-complexes to differ by at least 0.2 s and taking the largest maximum for local maxima closer than 0.2 s to each other as position of the QRS complex. Afterward, we cut potentially overlapping 0.48 s-windows centered around the QRS-complexes from the acceleration signal and compute a list of correlation values between each window with each other. If characteristic acceleration patterns can be linked to the QRS-complexes, the correlation between these windows should be large, whereas we expect them to be small else. Taking the 75-th percentile of this list gives us a correlation feature v_8 for arrhythmic rhythms. Employing the 75-th percentile instead of the mean balances well between correlation values that are high by coincidence and not taking windows with artifacts in the acceleration signal into account. In the case of ECG rhythms with no QRS-complexes, the algorithm still finds peaks with steep slopes and uses them for further processing. Since physiologically no accelerations by the apex beat should be detectable for these rhythms, the acceleration signals of the windows around those peaks should be uncorrelated to each other regardless of what peak the algorithm has detected.

For the ECG we further use the features $(v_9, \dots, v_{14}) = (P_{LEA}, L_{\min}, b_S, n_P, F_{\text{fib}}, P_h)$ which were computed following [22]. We do not employ features proposed in the literature for PR/PEA discrimination, since our data contain other rhythms (like ventricular fibrillation or pulseless ventricular tachycardia) too, for which these features, mainly based on QRS-complex detection, might fail. These 14 features and the label can be represented as $(\mathbf{x}, y) \in \mathbb{R}^{14} \times \{-1, 1\}$, where

$y = +1$ is related to SC and $y = -1$ with its absence. We refer to v_1, v_3, v_5, v_6, v_7 and v_8 as 'ACC-features', and call the remaining features 'ECG-features'. Note that ECG-features use solely ECG data, whereas ACC-features employ ACC data or a combination of ACC and ECG. Capnography data are only used for prefiltering, but remain unused in our features.

2.4 Learning/Training

The total data set (\mathbf{x}, y) was randomly split into a training set $(\mathbf{x}_{\text{train}}, y_{\text{train}})$ and a test set $(\mathbf{x}_{\text{test}}, y_{\text{test}})$. The set sizes follow a ratio of 0.8 : 0.2. The training data were shifted to median 0 and scaled to interquartile range 1, and the same transformation was applied to the test set. The training set was used to train a Gaussian kernel (rbf) Support Vector Machine (SVM) classification model with l_2 -regularization using the package SciKit-Learn [23] which employs LIBSVM package [24]. The optimal hyperparameters (kernel parameter γ and regularization C) were chosen to maximize the accuracy during 3-fold cross-validation. The performance of the model was assessed using accuracy, sensitivity, specificity, and Mathew's correlation coefficient (MCC) on the test set. SciKit-Learn [23] additionally assigns every prediction a class probability. We trained models on data sets with and without capnography prefiltering and using all available features or only parts of the available features to determine the influence of different feature subsets and the capnography prefiltering on the performance of the classifier. The confidence intervals for accuracy, sensitivity, and specificity are computed by the normal approximation to the binomial distribution. The confidence intervals on the MCC are calculated by employing Fisher's z-transform [25]. All performance measures are given as value (95%-confidence interval). The code for the classifier and the scaler using all features trained on capnography-prefiltered data, together with 5 exemplary cases is made publicly available in [26].

3 Results

From the total sample of 917 cases, 87 recordings were excluded from further analysis since the files were corrupted, for 33 cases no conclusive annotation was feasible, and in 164 cases no simultaneous ECG, ACC, and capnography signals were available. 124 of the remaining cases lack interruptions in CPR with appropriate length or lack signal overlap before the end of the last chest compression period. So a total of 509 cases was included, yielding 39924 snippets (19829 AR and 20095 SC). When applying both general and capnography prefiltering conditions, only 14830 snippets (7653 AR and 7177 SC) from 378 cases are included in the analysis, whereas 27451 (12900 AR and 14551 SC) snippets from 488 cases are left in case of general prefiltering only.

3.1 Overall Results

The best classifier ($C = 4.5, \gamma = 0.6$) on the data set with capnography prefiltering yielded a sensitivity of 95.0 (93.9, 96.1)% a specificity of 93.9 (92.7, 95.1)%, an accuracy of 94.4 (93.6, 95.2)% and a MCC of 0.888 (0.880, 0.895) on the test set and a sensitivity of 98.9 (98.6, 99.1)% a specificity of 99.4 (99.1, 99.6)%, an accuracy of 99.1 (99.0, 99.3)% and a MCC of 0.982 (0.981, 0.983) on the training set. Note that the application of capnography prefiltering mitigates the shortcomings of the annotation process described above.

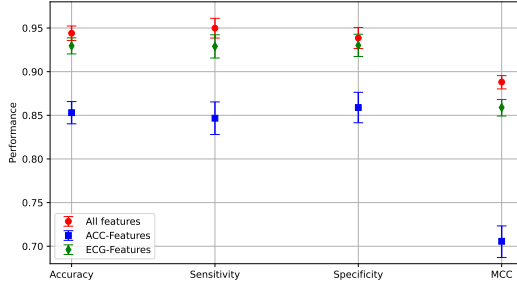


Figure 3: Classifier performance for different subsets of features on the capnography prefiltered set. Using ECG features solely performs better than using ACC features solely. A combination of both feature subsets enhances performance considerably.

Table 1: Classifier performance on data set with capnography prefiltering

	All features	ACC-features	ECG-features
Accuracy	94.4 % (93.6, 95.2) %	85.3 % (84.0, 86.6) %	93.0 % (91.6, 93.9) %
Sensitivity	95.0 % (93.9, 96.1) %	84.7 % (82.8, 86.5) %	92.9 % (91.6, 94.2) %
Specificity	93.9 % (92.7, 95.1) %	85.9 % (84.1, 87.6) %	93.0 % (91.7, 94.3) %
MCC	0.888 (0.880, 0.895)	0.706 (0.687, 0.723)	0.859 (0.849, 0.868)

3.2 Detailed Results

To determine the contribution of novel ACC-features to the overall performance, we trained models using either ACC-features ($C = 6, \gamma = 0.6$) or ECG-features ($C = 4, \gamma = 2.1$) too and compared them to the general model. The performance measures are given in Table 1. Although using only ECG-features performs well, adding acceleration features improves the classification result. The classification performance depending on the employed features is also illustrated in Fig. 3.

Furthermore, we trained a model also on the data set without capnography prefiltering ($C = 3.5, \gamma = 0.7$). The performance for ACC features ($C = 6.5, \gamma = 0.3$) and ECG features ($C = 9, \gamma = 1.75$) was analyzed for this larger set too and all performance measures are given in Table 2 and Fig. 4. The performance of the algorithm trained on the general data set is inferior to the one with capnography prefiltering, indicating possible insufficiency of the annotation process, but as before, all performance measures, particularly specificity, are enhanced by adding ACC-features. Hence, the acceleration data provide additional information to classify a snippet as 'Cardiac Arrest' correctly, which otherwise would have been falsely predicted as 'Spontaneous Circulation' by ECG-features only. This could be related to the differentiation between PR, pseudo-PEA, and true-PEA, for which ECG rhythms look similar, but cardiac output differs.

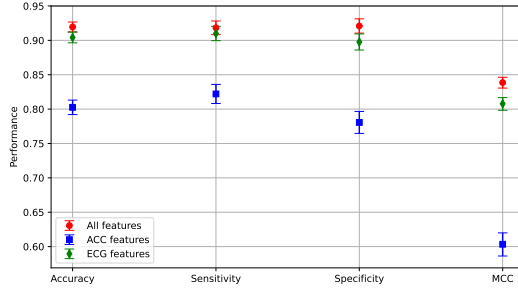


Figure 4: Classifier performance for different subset features for general prefiltering only. The performance is worse than for data with capnography prefiltering. Nevertheless, performance increases when using all features.

Table 2: Classifier performance on data set with general prefiltering only

	All features	ACC-features	ECG-features
Accuracy	92.0 % (91.2, 92.7) %	80.3 % (79.2, 81.3) %	90.4 % (89.6, 91.2) %
Sensitivity	91.8 % (90.8, 92.8) %	82.2 % (80.8, 83.6) %	91.0 % (90.0, 92.0) %
Specificity	92.1 % (91.1, 93.1) %	78.1 % (76.5, 79.7) %	89.8 % (88.6, 90.9) %
MCC	0.839 (0.831, 0.846)	0.603 (0.582, 0.620)	0.808 (0.798, 0.817)

3.3 Misclassifications

Analyzing exemplary misclassified snippets provides insight into possible causes of misclassification. In Fig. 5 we see examples of 3 consecutive snippets covering a total length of 8 seconds with prediction, probability of prediction, and ground truth below. All snippets are from the test set unseen in training. Fig. 5a contains clear QRS-complexes in the ECG and clearly related acceleration excitations. The algorithm classifies correctly all snippets shown with high probability as SC. In Fig. 5b, no acceleration excitations can be related to the distinctly visible QRS-complexes. Consistently, all snippets are predicted as AR. In Fig. 5c the central snippet, which is exhibiting regularly looking accelerations of unknown source synchronous to the QRS-complexes, is falsely classified as SC. In Fig. 5d, where the acceleration excitations from the apex beat are covered by the large-amplitude noise, the central snippet is predicted falsely as AR. For both misclassified snippets, noise is comparatively large. Additionally, in Fig. 5d the ECG is highly arrhythmic. By inspecting both signals closer, acceleration excitations can not be related biuniquely to QRS-complexes. While some ECG peaks lead to clear acceleration peaks, for other QRS-complexes, no respective acceleration signal is found. Besides the open question whether no apex beat is present for these extrasystoles, or its presence was not detected by the accelerometer, these extrasystoles with missing acceleration peaks cause additional complications for a reliable circulation detection algorithm based on ACC since the arrhythmic correlation feature v_8 might fail then too.

3.4 Case Studies

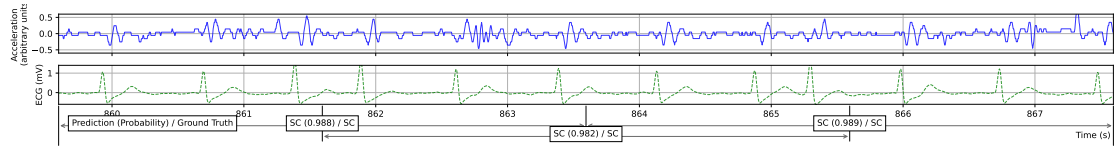
Further information about the performance of the algorithm can be gained by plotting the predictions and their probability of successive snippets over time. In Fig. 6, two exemplary situations are shown. In Fig. 6a, the QRS-complexes get sparser over time, and also acceleration peaks decrease. The algorithm predicts the probability of spontaneous circulation to be below 50% at least 15 s earlier than retrospectively annotated. Due to this slow deceleration of heart rate, defining an exact arrest time is unfeasible here. In Fig. 6b the arrest time can be defined unambiguously by the abrupt rhythm change in ECG. Correspondingly, the algorithm predicts AR subsequently. After the shock, the organized rhythm starts again, and the algorithm predicts SC with high probability.

The performance of the classifier on 5 different cases is furthermore illustrated in [26].

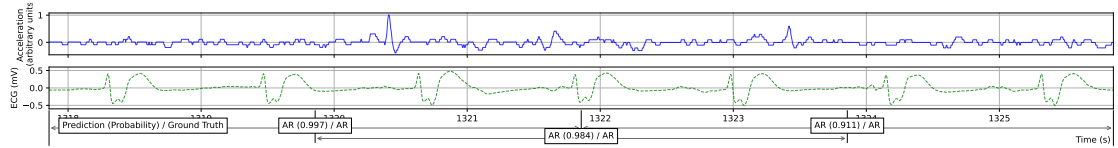
4 Discussion

To the best of our knowledge, this study is the first to employ accelerometry data to classify the circulatory state in cases of out-of-hospital cardiac arrest treatment. The proposed algorithm shows excellent performance measures on the data set prefiltered by capnography and respectable performance on the general data set. In contrast to other studies investigating seismocardiography in porcine models [16] or under lab conditions [17], this work employs retrospective analysis of prospectively collected real-world data from defibrillator recordings, leading to conceptual advantages on the one hand, but causing disadvantages on the other hand too.

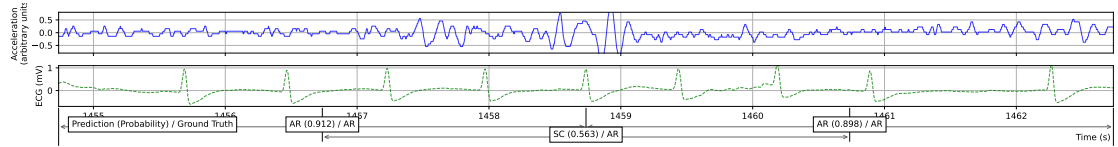
Using real-world recordings demonstrates the applicability of seismocardiography to assess the circulatory state also on noisy signals from the field. Although the main purpose of the defibrillator models' accelerometer used in this study is the assessment of CPR quality delivered by the EMS, the apex beat is still detectable by these devices. However, since acceleration amplitudes by the apex beat are comparatively small, discretization artifacts are already visible in the recordings, and inevitable noise and artifacts from the transport or medical treatment cover



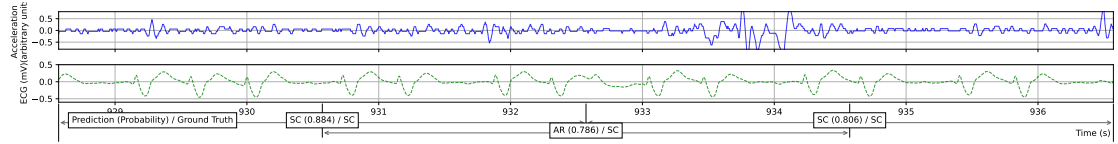
(a) True positive prediction



(b) True negative prediction



(c) False positive prediction



(d) False negative prediction

Figure 5: Four exemplary situations consisting of 3 overlapping snippets from test data containing a total signal length of 8 seconds with real and predicted circulatory states with probability noted below (SC, AR). Acceleration signals are given in blue, ECG signals in green. The falsely predicted snippets were chosen from the data set so that they are pinched between two correct classifications in order to visualize changes in the signal leading to these misclassifications.

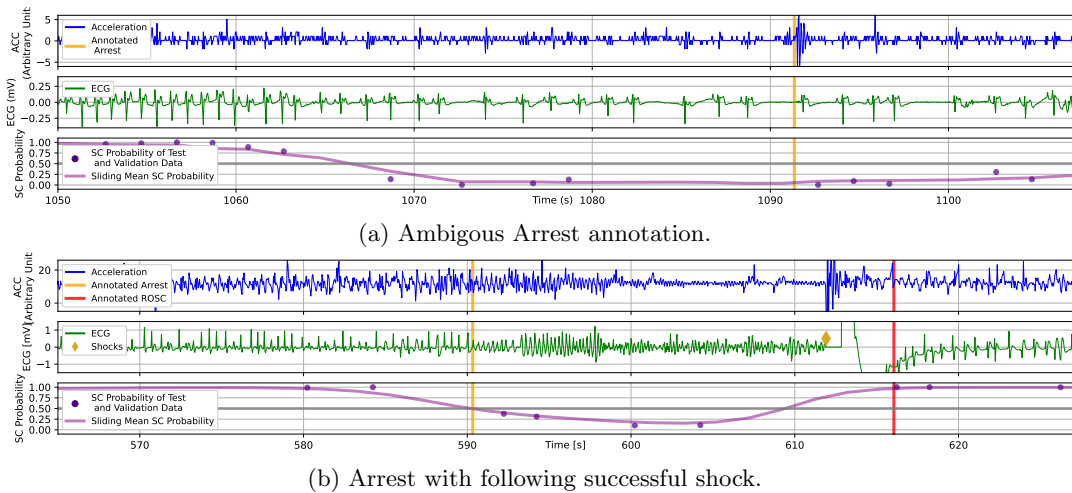


Figure 6: Two exemplary situations with predicted spontaneous circulation probabilities over time. Acceleration data (blue), ECG data (green) and probabilities (purple scatters), and a sliding mean of probabilities (purple solid line) are given. Additionally, the labels by the manual, retrospective annotation and the time of the shock (yellow diamonds) are shown. Only snippets from test set are shown in the plots. Note the polymorphic ventricular extrasystoles in 6b.

the signal easily and complicate analysis. Furthermore, the defibrillator recordings from cardiac arrest patients contain data from ischemic hearts where inotropy might be reduced, wall motion abnormalities may be present and subsequently signal quality might be worse than for healthy patients. Moreover, the accelerometer is placed directly on the sternum of the patient and the measuring range of the accelerometer is adjusted to accelerations occurring in CPR. Using devices with measuring ranges adapted to the expected signal strength and optimizing the position of the accelerometer on the chest - possibly in the apical shock electrode - could improve signal quality considerably. Even though the best configuration requires further investigation. Still, the respectable performance of the algorithm demonstrates its applicability in the current configuration too.

One key difficulty of our data collection is the determination of a reliable ground truth. Retrospective annotation of the circulatory state is inevitably imprecise for several reasons. First, the annotators have to assess the circulatory state based on limited information provided by recordings and documentation so that a concluding annotation might not be feasible. We tried to encounter this problem by assuming faultless treatment by the EMS and exclusion of obtuse intervals during the annotation process. Second, the dichotomous annotation design does not take account of periarrest situations like pseudo-PEA, where cardiac contraction is present but insufficient. These situations can not be classified unambiguously within this framework. Since the heart is also palpating in pseudo-PEAs our algorithm could still be capable of detecting the apex beat, even if cardiac output is insufficient. We roughly addressed this problem by applying additional capnography prefiltering which aims to exclude periarrest situations by requiring certain endtidal CO_2 concentration levels from our analysis. A better assessment of periarrest rhythms requires more intricate measurements of cardiac output like echocardiography or invasive arterial blood pressure, which are not present in our data set. Employing such measurements could further investigate the question of whether seismocardiography is capable of assessing the circulatory state not only qualitatively but also quantifying cardiac contractility which has to

remain unanswered due to a lack of appropriate data.

Finally, only one year was annotated by two independent physicians, where dissenting annotations were resolved in consensus. The rest of the data were labeled by a single physician. In addition, all data were collected from one model (ZOLL X-Series) in this study. However, as long as the accelerometer records with at least similar resolution and appropriate sample rate and its position is adequate to record the apex beat, the same working principle should be applicable to other models too.

In contrast to other circulation classification algorithms proposed in the literature, this algorithm operates on a more general data set containing not only organized (PR and PEA), but also any other ECG rhythms where mechanical decoupling can be assessed directly from ECG data (e.g. ventricular fibrillation or asystole). This is mirrored by the fact that using only ECG features for analysis yields already good classification results. Nevertheless, adding information from the accelerometer increases classification performance considerably. Furthermore, the acceptance of any ECG and acceleration signal pair as input allows for an application in more general situations with pulse generating arrhythmias present. Due to this broader data set, a comparison of our algorithm to other results remain inconclusive. In the porcine model by Wei et al. [16] employing accelerometry exhibited a sensitivity of 93.6% and a specificity of 97.5% to discriminate PEA from PR under lab conditions. They proposed the usage of a peak cross-correlation between filtered ECG and ACC signals as single feature in their work. Due to inevitable noise in our data this feature was not used as an input.

Compared to the usage of thoracic impedance [11, 9] seismocardiography exhibits a big advantage: While ventilation and respiration induce large amplitude signals in thoracic impedance [9], potentially complicating circulatory state assessment, the slow movement of the chest wall during ventilation or respiration is hardly detectable in the acceleration signal.

Regarding applicability in real-world cardiac arrest treatment, one could additionally exploit the chronological order of the snippets. So far, the algorithm does not include the snippets' temporal information since they get thoroughly mixed up and split into different data sets before training. The prediction of a circulatory state of a single snippet does not take the state of the previous or next snippet into account. However, in real-world, consecutive snippets will mostly be related to each other since circulatory state transitions do not take place every few seconds normally, allowing for an identification of single misclassifications.

Employing temporal information is also relevant to assess the medical practicality of this algorithm in the field. During cardiac arrest treatment, a quick and reliable recognition of circulatory state changes is necessary to reduce no-flow time. The capability of the algorithm to detect ROSC and rearrest events within a short time interval on unknown cases needs further investigation in order to evaluate its usefulness as a support tool. Additionally, our splitting of the data into training and test cases so far did not take into account the association of different time snippets to different patients. Splitting the data on a patient-basis will be necessary for a real-world application of our algorithm in the field, but can be expected to cause additional difficulties for classification, due to inter-individual factors.

Besides the usage of the algorithm in the field during cardiac arrest treatment, another purpose is the retrospective analysis. Currently, manual annotation is necessary to evaluate key CPR quality metrics like chest compression fraction. While recent works [19, 20, 21, 27] proposed methods how to compute the time with ongoing chest compressions automatically, the length of the cardiac arrest intervals still needs manual annotation. Our proposed algorithm could facilitate manual annotation by suggesting appropriate intervals, which physicians only need to approve instead of single-handed analyzing the whole case in detail. This assistance could allow for broader application of CPR quality metrics in general registries [28].

5 Conclusion

This study presented a machine learning algorithm using ECG and ACC data to determine the circulatory state of cardiac arrest patients. This algorithm could serve as a valuable medical decision tool to provide optimal treatment for cardiac arrest data.

References

- [1] Jan-Thorsten Gräsner, Johan Herlitz, Ingvild B.M. Tjelmeland, Jan Wnent, Siobhan Masterson, Gisela Lilja, Berthold Bein, Bernd W. Böttiger, Fernando Rosell-Ortiz, Jerry P Nolan, Leo Bossaert, and Gavin D. Perkins. European resuscitation council guidelines 2021: Epidemiology of cardiac arrest in europe. *Resuscitation*, 161:61–79, 2021.
- [2] F Javier Ochoa, E Ramalle-Gomara, JM Carpintero, A Garcia, and I Saralegui. Competence of health professionals to check the carotid pulse. *Resuscitation*, 37(3):173–175, 1998.
- [3] B. Eberle, W.F. Dick, T. Schneider, G. Wisser, S. Doetsch, and I. Tzanova. Checking the carotid pulse check: diagnostic accuracy of first responders in patients with and without a pulse. *Resuscitation*, 33(2):107–116, 1996.
- [4] Jim Christenson, Douglas Andrusiek, Siobhan Everson-Stewart, Peter Kudenchuk, David Hostler, Judy Powell, Clifton W Callaway, Dan Bishop, Christian Vaillancourt, Dan Davis, et al. Chest compression fraction determines survival in patients with out-of-hospital ventricular fibrillation. *Circulation*, 120(13):1241–1247, 2009.
- [5] Jasmeet Soar, Bernd W. Böttiger, Pierre Carli, Keith Couper, Charles D. Deakin, Therese Djärv, Carsten Lott, Theresa Olasveengen, Peter Paal, Tommaso Pellis, Gavin D. Perkins, Claudio Sandroni, and Jerry P. Nolan. European resuscitation council guidelines 2021: Adult advanced life support. *Resuscitation*, 161:115–151, 2021. European Resuscitation Council Guidelines for Resuscitation 2021.
- [6] Andoni Elola, Elisabete Aramendi, Unai Irusta, Javier Del Ser, Erik Alonso, and Mohamud Daya. Ecg-based pulse detection during cardiac arrest using random forest classifier. *Medical & biological engineering & computing*, 57(2):453–462, 2019.
- [7] Andoni Elola, Elisabete Aramendi, Unai Irusta, Artzai Picón, Erik Alonso, Pamela Owens, and Ahamed Idris. Deep neural networks for ecg-based pulse detection during out-of-hospital cardiac arrest. *Entropy*, 21(3):305, 2019.
- [8] Nick Alexander Cromie, John Desmond Allen, Colin Turner, John McC Anderson, and A A Jennifer Adgey. The impedance cardiogram recorded through two electrocardiogram/defibrillator pads as a determinant of cardiac arrest during experimental studies. *Critical care medicine*, 36(5):1578–1584, 2008.
- [9] Andoni Elola, Elisabete Aramendi, Unai Irusta, Artzai Picón, Erik Alonso, Iraia Isasi, and Ahamed Idris. Convolutional recurrent neural networks to characterize the circulation component in the thoracic impedance during out-of-hospital cardiac arrest. In *2019 41st Annual International Conference of the IEEE Engineering in Medicine and Biology Society (EMBC)*, pages 1921–1925. IEEE, 2019.
- [10] Martin Risdal, Sven Ole Aase, Jo Kramer-Johansen, and Trygve Eftestol. Automatic identification of return of spontaneous circulation during cardiopulmonary resuscitation. *IEEE Transactions on Biomedical Engineering*, 55(1):60–68, 2008.

- [11] Erik Alonso, Elisabete Aramendi, Mohamud Daya, Unai Irusta, Beatriz Chicote, James K. Russell, and Larisa G. Tereshchenko. Circulation detection using the electrocardiogram and the thoracic impedance acquired by defibrillation pads. *Resuscitation*, 99:56–62, 2016.
- [12] Jesus M. Ruiz, Sofía Ruiz de Gauna, Digna M. González-Otero, Purificación Saiz, J. Julio Gutiérrez, Jose F. Veintemillas, Jose M. Bastida, and Daniel Alonso. Circulation assessment by automated external defibrillators during cardiopulmonary resuscitation. *Resuscitation*, 128:158–163, 2018.
- [13] Andoni Elola, Elisabete Aramendi, Unai Irusta, Erik Alonso, Yuanzheng Lu, Mary P Chang, Pamela Owens, and Ahamed H Idris. Capnography: A support tool for the detection of return of spontaneous circulation in out-of-hospital cardiac arrest. *Resuscitation*, 142:153–161, 2019.
- [14] Ralph W. C. G. R. Wijshoff, Antoine M. T. M. van Asten, Wouter H. Peeters, Rick Bezemer, Gerrit Jan Noordergraaf, Massimo Mischi, and Ronald M. Aarts. Photoplethysmography-based algorithm for detection of cardiogenic output during cardiopulmonary resuscitation. *IEEE Transactions on Biomedical Engineering*, 62(3):909–921, 2015.
- [15] Allison L. Cohen, Timmy Li, Lance B. Becker, Casey Owens, Neha Singh, Allen Gold, Mathew J. Nelson, Daniel Jafari, Ghania Haddad, Alexander V. Nello, Daniel M. Rolston, Cristina Sison, and Martin L. Lesser. Femoral artery doppler ultrasound is more accurate than manual palpation for pulse detection in cardiac arrest. *Resuscitation*, 173:156–165, 2022.
- [16] Liang Wei, Gang Chen, Zhengfei Yang, Tao Yu, Weilun Quan, and Yongqin Li. Detection of spontaneous pulse using the acceleration signals acquired from cpr feedback sensor in a porcine model of cardiac arrest. *PLOS ONE*, 12(12):1–11, 12 2017.
- [17] Hyoung Youn Lee, Yong Hun Jung, Kyung Woon Jeung, Dong Hun Lee, Byung Kook Lee, Geuk Young Jang, Tong In Oh, Najmiddin Mamadjonov, and Tag Heo. Discrimination between the presence and absence of spontaneous circulation using smartphone seismocardiography: A preliminary investigation. *Resuscitation*, 166:66–73, 2021.
- [18] Thomas Kluyver, Benjamin Ragan-Kelley, Fernando Pérez, Brian Granger, Matthias Bussonnier, Jonathan Frederic, Kyle Kelley, Jessica Hamrick, Jason Grout, Sylvain Corlay, Paul Ivanov, Damián Avila, Safia Abdalla, and Carol Willing. Jupyter notebooks – a publishing format for reproducible computational workflows. In F. Loizides and B. Schmidt, editors, *Positioning and Power in Academic Publishing: Players, Agents and Agendas*, pages 87 – 90. IOS Press, 2016.
- [19] Jo Kramer-Johansen, Dana P Edelson, Heidrun Losert, Klemens Köhler, and Benjamin S Abella. Uniform reporting of measured quality of cardiopulmonary resuscitation (cpr). *Resuscitation*, 74(3):406–417, 2007.
- [20] Simon Orlob, Wolfgang J. Kern, Birgitt Alpers, Michael Schörghuber, Andreas Bohn, Martin Holler, Jan-Thorsten Gräsner, and Jan Wnent. Chest compression fraction calculation: A new, automated, robust method to identify periods of chest compressions from defibrillator data – tested in zoll x series. *Resuscitation*, 2022.
- [21] Wolfgang J. Kern, Simon Orlob, Birgitt Alpers, Michael Schörghuber, Andreas Bohn, Martin Holler, Jan-Thorsten Gräsner, and Jan Wnent. A sliding-window based algorithm

- to determine the presence of chest compressions from acceleration data. *Data in Brief*, page 107973, 2022.
- [22] Unai Ayala, U Irusta, J Ruiz, T Eftestøl, J Kramer-Johansen, F Alonso-Atienza, E Alonso, and D González-Otero. A reliable method for rhythm analysis during cardiopulmonary resuscitation. *BioMed research international*, 2014, 2014.
- [23] F. Pedregosa, G. Varoquaux, A. Gramfort, V. Michel, B. Thirion, O. Grisel, M. Blondel, P. Prettenhofer, R. Weiss, V. Dubourg, J. Vanderplas, A. Passos, D. Cournapeau, M. Brucher, M. Perrot, and E. Duchesnay. Scikit-learn: Machine learning in Python. *Journal of Machine Learning Research*, 12:2825–2830, 2011.
- [24] Chih-Chung Chang and Chih-Jen Lin. LIBSVM: A library for support vector machines. *ACM Transactions on Intelligent Systems and Technology*, 2:27:1–27:27, 2011. Software available at <http://www.csie.ntu.edu.tw/~cjlin/libsvm>
- [25] Ronald A Fisher. Frequency distribution of the values of the correlation coefficient in samples from an indefinitely large population. *Biometrika*, 10(4):507–521, 1915.
- [26] Wolfgang J. Kern, Simon Orlob, and Martin Holler. Cprdat, September 2021. Dataset will be updated with classifiers after acceptance of this publication.
- [27] Vishal Gupta, Robert H Schmicker, Pamela Owens, Ava E Pierce, and Ahamed H Idris. Software annotation of defibrillator files: ready for prime time? *Resuscitation*, 160:7–13, 2021.
- [28] Xabier Jaureguibeitia, Elisabete Aramendi, Unai Irusta, Erik Alonso, Tom P. Aufderheide, Robert H. Schmicker, Matthew Hansen, Robert Suchting, Jestin N. Carlson, Ahamed H. Idris, and Henry E. Wang. Methodology and framework for the analysis of cardiopulmonary resuscitation quality in large and heterogeneous cardiac arrest datasets. *Resuscitation*, 168:44–51, 2021.